Section: Radiation Oncology

Original Research Article

DOSIMETRIC CHARACTERIZATION OF AL_2O_3:C NANODOT OPTICALLY STIMULATED LUMINESCENCE DOSIMETERS IN THERAPEUTIC PHOTON BEAMS

Nanda Kumar M[1], MG. Giriyappagoudar[2], Savitha AK[3], Shashikala N[4]

[1]*Medical physicist & Radiation Safety Officer, Department of Radiation Oncology, Apollo BGS Hospital, Mysore, Karnataka, India.*
[2]*Associate Professor, Department of Radiation Oncology, Karnataka Medical College and Research Institute, Hubballi, Karnataka, India.*
[3]*Assistant Professor, Department of General Medicine, Shivamogga Institute of Medical Sciences, Shivamogga, Karnataka, India.*
[4]*Medical Physicist, Department of Radiation Oncology, Kidwai Memorial Institute of Oncology, Bangalore, Karnataka, India.*

Received *: 04/08/2026*
Received in revised form *: 26/08/2026*
Accepted *: 08/09/2026*

Corresponding Author:
Dr. Shashikala N,
Medical Physicist, Department of Radiation Oncology, Kidwai Memorial Institute of Oncology, Bangalore, Karnataka, India.
Email: shashinandan1617@gmail.com

DOI: 10.70034/ijmedph.2026.3.742

Source of Support: Nil,
Conflict of Interest: None declared

Int J Med Pub Health
2026; 16 (3); 4808-4814

ABSTRACT

Background: Carbon-doped aluminum oxide optically stimulated luminescence dosimeters (Al_2O_3:C OSLDs) combine high sensitivity, small dimensions and repeated optical readout, but their response must be characterized before radiotherapy use. The objective is to evaluate nano Dot OSLD element correction factors, dose response, field-size and dose-rate dependence, reproducibility, signal depletion and angular dependence in therapeutic photon beams.

Materials and Methods: Detectors were irradiated in solid-water phantoms with ^{60}Co and 6-, 15- and 18-MV photon beams, including a 6-MV flattening-filter-free beam. Dose response was studied from 50 to 1,000 cGy, field size from 3 × 3 to 30 × 30 cm², dose rate from 100 to 600 MU/min, repeated readout through 200 measurements, and angular response from 0° to 350°. A Farmer-type ionization chamber provided reference measurements where applicable.

Results: Element correction factors ranged from 0.91 to 1.08, with 88% of detectors within 5% of the batch mean. Response was linear from 50 to 300 cGy (R^2 = 0.993-0.997) and supralinear above 300 cGy. Field-size differences were 1.22%-1.60%, and dose-rate differences reached 1.8%. Inter-detector variation was below 1.06%. Signal loss was 0.06%-0.07% per readout, while angular deviation reached 6%.

Conclusion: nanoDot OSLDs provided reproducible point-dose measurements within the validated range. Individual sensitivity correction, controlled orientation, standardized reuse and dose-specific calibration are required for clinical implementation.

Keywords: optically stimulated luminescence; nanoDot; Al_2O_3:C; radiotherapy dosimetry; photon beams; quality assurance; in vivo dosimetry

INTRODUCTION

Accurate absorbed-dose verification is essential in external-beam radiotherapy because differences between planned and delivered dose can arise from calibration, equipment performance, data transfer, phantom positioning, or detector placement. Independent point measurements remain valuable even when treatment-planning systems and delivery devices undergo comprehensive quality assurance. A clinically useful detector should provide adequate sensitivity and spatial resolution, stable response, manageable uncertainty, and practical handling without materially disturbing the radiation field. Contemporary guidance therefore treats luminescent dosimetry as a commissioned measurement system rather than a detector that can be used with a universal calibration.[1]

Optically stimulated luminescence dosimetry estimates absorbed dose from light emitted when an irradiated phosphor is exposed to a controlled optical stimulus. Ionizing radiation traps charge carriers at defects within the crystal lattice; stimulation releases part of the stored energy as luminescence, and the measured signal is related to absorbed dose. Carbon-doped aluminum oxide (Al_2O_3:C) is attractive

because of its high sensitivity, broad usable range, and ability to retain sufficient signal for repeated readings. Unlike thermoluminescent dosimeters, it does not require heating during measurement, which simplifies handling and allows reanalysis when a reading must be confirmed.[2]

The commercial nanoDot format encloses a small Al_2O_3:C disk within a labeled, light-tight plastic cassette. Its compact dimensions suit phantom point measurements and locations where larger ionization chambers provide inadequate spatial resolution. However, the photomultiplier-tube signal depends on more than absorbed dose. Manufacturing variation produces detector-specific sensitivity differences; optical stimulation gradually removes stored signal; accumulated irradiation and bleaching history can affect reuse; and response may change with energy, dose, and cassette orientation. Current development of OSL materials continues to emphasize sensitivity, stability, linearity, fading, and reproducible readout as connected performance requirements.[3]

Recent literature further demonstrates why application-specific testing is necessary. Reviews of photonic radiation detectors identify OSL systems as versatile but calibration-dependent technologies.[4] Characterization in cobalt-60 high-dose-rate fields has documented dose, energy, and geometry effects that require local evaluation.[5] Exit-dose studies have also shown the clinical potential of OSLDs when detector correction and placement are carefully controlled.[6] Flexible OSL detector arrays illustrate how the same physical principle can be extended to spatially resolved in vivo measurements.[7] Together, these findings make calibration range, cassette orientation, readout control, and traceable detector history central components of a defensible radiotherapy protocol.

The present study examined nanoDot OSLDs across ^{60}Co and megavoltage photon beams from two linear-accelerator platforms. The investigation addressed element correction factors, linear and supralinear dose response, field-size dependence, dose-rate dependence, short-term reproducibility, optical bleaching, accumulated dose, signal depletion during repeated readout, and angular dependence. Measurements were compared with a Farmer-type ionization chamber where matched reference data were available. The objective was to identify conditions under which nanoDot OSLDs can provide reliable point-dose measurements and determine the corrections or procedural controls required before routine phantom or in vivo application. Unresolved limitations involving detector count, beam grouping, replication, and uncertainty reporting were retained for transparent interpretation.

A further practical consideration is workflow standardization. Small deviations in the interval between irradiation and readout, number of repeated measurements, reader settings, optical bleaching duration, cassette position, or normalization method can obscure the dosimetric effect being investigated. Reporting these details is necessary for reproducibility across institutions. Characterization should also distinguish detector precision from agreement with a reference system, because a highly repeatable signal may still be biased. Accordingly, the present comparison evaluates both internal OSLD consistency and agreement with ionization-chamber measurements under matched phantom conditions while separating conventional-dose performance from high-dose, repeated-readout, reuse, and orientation effects. This structure supports transparent interpretation while preserving the measured relationships among absorbed dose, beam condition, handling history, cassette orientation, and readout sequence for clinicians.

MATERIALS AND METHODS

Study design and setting: This phantom-based investigation used radiotherapy equipment at Kidwai Cancer Institute, Bengaluru. No patients, biological samples, or identifiable information were involved. Irradiations employed a ^{60}Co unit and linear accelerators delivering 6-, 15-, and 18-MV flattened beams and a 6-MV flattening-filter-free beam. Experiments assessed individual sensitivity, dose response, field size, dose rate, reproducibility, readout depletion, and orientation. Individual sensitivity was evaluated because it can influence dose estimation.[8]

Dosimetry system and reference instrumentation: Commercial nanoDot OSLDs contained a 5-mm-diameter, 0.2-mm-thick Al_2O_3:C disk in a light-tight cassette. A microStar reader stimulated each disk and measured emitted light with a photomultiplier tube. For reuse, cassettes were opened and bleached under fluorescent light for six hours. Reference measurements used an FC65-G Farmer-type chamber, PC electrometer, solid-water slabs, and Perspex inserts. Detector identifiers were tracked through irradiation, bleaching, and readout. Comparable nanoDot calibration procedures have been reported for low-energy radiotherapy beams.[9]

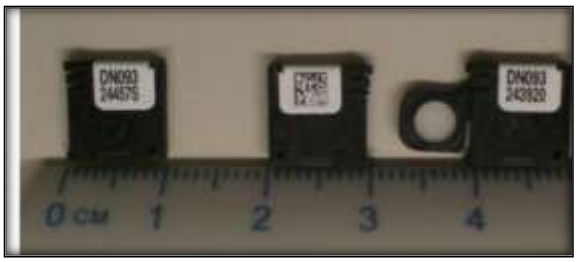

Figure 1: nanoDot OSL dosimeters, from left to right: front face with unique identification number, reverse face with barcode, and cassette opened to expose the white circular Al_2O_3:C detector element.

Reference irradiation geometry: Linear-accelerator irradiations used a 100-cm SSD, 10-cm depth, 10 × 10 cm² field, 400 MU/min, and 10 cm of backscatter. The ^{60}Co arrangement used an 80-cm SSD, 5-cm

depth, and the same field. OSLDs and the chamber occupied inserts under matched depth, field, and backscatter conditions. Placement was perpendicular to beam incidence except during angular testing. Geometry was controlled because nanoDot response can vary when irradiation conditions change.[10]

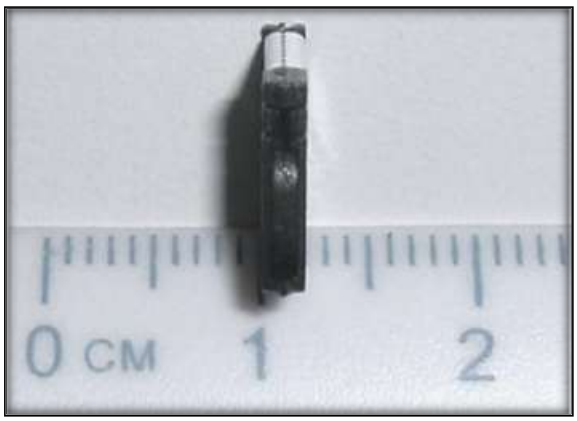

Figure 2: Edge-on view of a nanoDot OSLD demonstrating the approximately 2-mm cassette thickness.

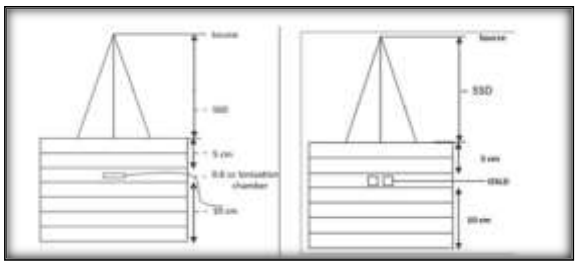

Figure 3: Reference irradiation geometry for matched measurements with (a) an ionization chamber and (b) nanoDot OSLDs positioned in the slab phantom.

Element correction factor: Individual sensitivity was corrected using an element correction factor (ECF). Two hundred OSLDs received a ^{60}Co dose; each was read three times. Each detector's mean net count was compared with the batch mean. ECF equalled mean batch count divided by individual detector count. Corrected signal equalled post-irradiation counts minus pre-irradiation count, multiplied by ECF. Background counts were recorded before calculation. Element-specific conversion similarly separates detector response from absorbed dose.[11]

ECF_i = mean batch PMT count / individual PMT $count_i$

Corrected OSL signal = (post-irradiation count - pre-irradiation count) × ECF_i

Dose response: Dose response was measured from 50 to 1,000 cGy, using 50-cGy steps through 400 cGy and 100-cGy steps thereafter. Measurements included ^{60}Co, Varian 6- and 18-MV beams, and Elekta 6-, 15-, and 6-MV FFF beams. OSLD and chamber responses were normalized at 200 cGy. Linear regression covered 50–300 cGy. From 400–1,000 cGy, supralinearity equalled observed response divided by prediction. Beam-specific results were retained, consistent with audit methods using defined conditions [12]

Field-size and dose-rate dependence: Field-size response was measured for fields from 3 × 3 to 30 × 30 cm² after 200 MU. OSLD and chamber factors were normalized to the 20 × 20 cm² field. Dose-rate dependence was examined for 6- and 18-MV beams from 100 to 600 MU/min in 100-MU/min increments. A fixed 200 MU was delivered, and responses were normalized to 400 MU/min. One factor changed within each comparison.

Reproducibility and readout depletion: Reproducibility was evaluated with four 2-Gy irradiations followed by bleaching, four 2-Gy irradiations without bleaching, and one 8-Gy irradiation. Readout began after 10 minutes. For depletion testing, detectors received 2 Gy or 10 Gy, stabilized for 30 minutes, and were measured 200 times. Loss per reading and cumulative loss at readings 50 and 200 were calculated relative to the response, separating repeatability from changes related to stimulation and accumulated dose.

Angular dependence: Angular dependence was tested for 6-MV flattened and FFF beams. Cassettes received 200 MU at angles from 0° through 350° in 10° increments. Focus-to-detector distance was 100 cm and SSD was 98.5 cm. Each result was normalized at 0°. No interpolation was applied, and orientation was recorded for every irradiation.

Data analysis: Analysis was descriptive and used normalized OSLD responses, determination coefficients, chamber differences, and signal loss. Results were grouped by beam and platform when possible. No inferential tests, confidence intervals, or complete uncertainty budgets were available; none were introduced. Detector-count, platform-assignment, and beam-coverage discrepancies were treated as limitations. Figures and tables present recorded numerical values, and normalizations retained the stated experimental reference conditions.

RESULTS

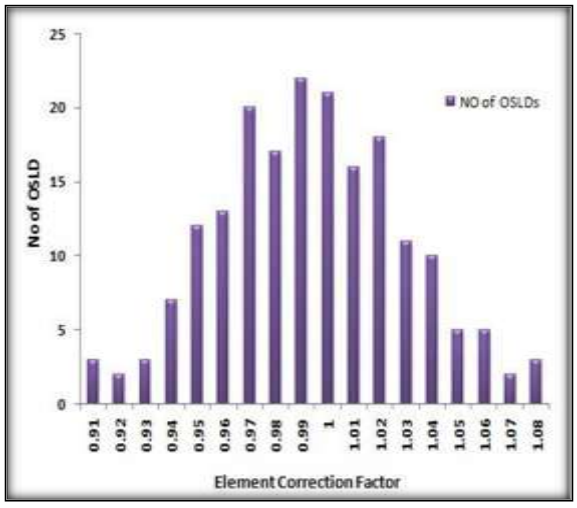

Figure 4: Distribution of element correction factors for the 200 evaluated nanoDot OSLDs.

Element correction factors: Element correction factors ranged from 0.91 to 1.08 across the 200-detector batch. The distribution was concentrated around unity, with the highest frequencies between approximately 0.97 and 1.02 (Figure 4). Overall, 88% of detectors showed sensitivity within 5% of the batch mean, and the remaining 12% were within 9%. The observed span represented a 17-percentage-point interval between the lowest and highest values. Applying one batch coefficient without individual correction would therefore transfer sensitivity variation into calculated dose. The ECF sequence was repeated three times before subsequent measurements to stabilize each assigned factor.

Dose response and supralinearity: Corrected OSLD response was linear from 50 to 300 cGy for every investigated beam. Coefficients of determination were 0.995 for ^{60}Co, 0.997 for Varian 6 MV, 0.994 for Varian 18 MV, 0.997 for Elekta 6 MV, 0.993 for Elekta 15 MV, and 0.996 for Elekta 6-MV FFF. All exceeded 0.99 within the interval. Above 300 cGy, response increased faster than linear-model prediction. At 1,000 cGy, supralinearity factors were 1.23, 1.21, 1.41, 1.28, 1.46, and 1.29 for the same beams, respectively [Table 1]. Elekta 15 MV produced the largest effect, whereas Varian 6 MV produced the smallest.

Table 1: Dose linearity and high-dose supralinearity reported for each photon beam. FFF, flattening-filter-free.

Beam / platform	R^2 (50-300 cGy)	Supralinearity factor at 1,000 cGy
^{60}Co / Telecobalt	0.995	1.23
6 MV / Varian	0.997	1.21
18 MV / Varian	0.994	1.41
6 MV / Elekta	0.997	1.28
15 MV / Elekta	0.993	1.46
6 MV FFF / Elekta	0.996	1.29

Field-size and dose-rate dependence: Across square fields from 3 × 3 to 30 × 30 cm², normalized OSLD output factors followed ionization-chamber trends. Maximum discrepancies were 1.5% for a 6-MV beam, 1.22% for 18 MV, 1.6% for 15 MV, and 1.4% for 6-MV FFF. All remained below 2%. Two 6-MV accelerator platforms were included, but independent maxima were unavailable for each platform. Dose-rate measurements also showed limited variation. From 100 to 600 MU/min, after normalization at 400 MU/min, the largest OSLD–chamber differences were 1.3% for 6 MV and 1.8% for 18 MV. Field-size and dose-rate effects were smaller than high-dose or orientation effects.

Reproducibility: Short-term inter-detector variation was below 1.06% under matched conditions. Detector-use history produced a larger change than immediate repeatability. The maximum difference between detectors bleached between exposures and detectors carrying accumulated dose was 8% for 6 MV and 9% for 18 MV. When the same exposure was delivered as one 8-Gy irradiation, the accumulated-dose effect was below 3%. Response therefore depended on the sequence of irradiation, readout, and bleaching as well as total dose. These findings support a detector-history record and consistent bleaching schedule for reused nanoDots.

Signal depletion during repeated readout: Repeated microStar measurements progressively depleted stored luminescence. Mean loss per readout was 0.06% after 2 Gy and 0.07% after 10 Gy. At reading 50, cumulative losses after 2 Gy were 3.6% for 6 MV and 3.2% for both 15 and 18 MV. After 10 Gy, values were 4.5%, 4.4%, and 5.0%. At reading 200, losses after 2 Gy reached 11%, 10%, and 15%, respectively; after 10 Gy, they reached 14%, 13%, and 18% [Table 2] The greatest depletion occurred for 18 MV after 10 Gy. Although loss per reading was small, repeated measurements produced meaningful cumulative change.

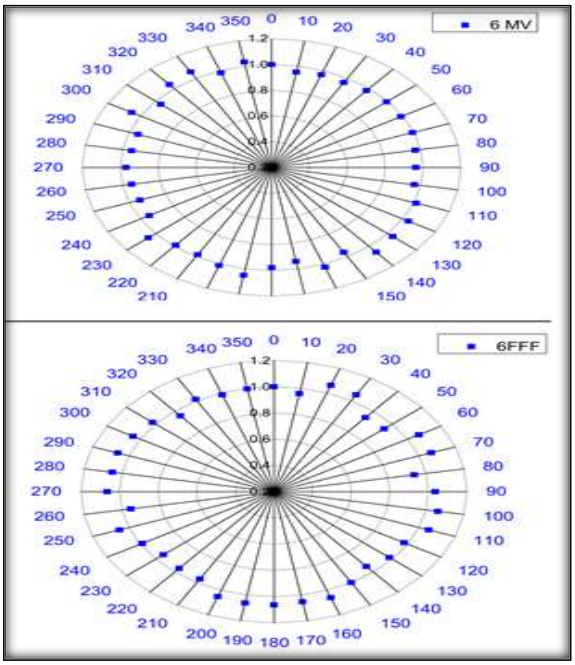

Figure 5: Angular response of nanoDot OSLDs for (a) a 6-MV flattened photon beam and (b) a 6-MV FFF photon beam, normalized to the response at 0°.

Table 2: Cumulative signal depletion during repeated microStar readout.

Beam	Loss at read 50, 2 Gy	Loss at read 50, 10 Gy	Loss at read 200, 2 Gy	Loss at read 200, 10 Gy
6 MV	3.6%	4.5%	11%	14%
15 MV	3.2%	4.4%	10%	13%
18 MV	3.2%	5.0%	15%	18%

Angular dependence: Angular measurements demonstrated systematic dependence on cassette orientation [Figure 5] For the 6-MV flattened beam, the maximum departure from response normalized at 0° was 5%, occurring at 250°. For the 6-MV FFF beam, maximum deviation was 6%, observed at 70° and 270°. Response changed around the full rotation rather than at one angle. The 6-MV FFF maximum was approximately one percentage point greater than that of the flattened beam. Angular variation exceeded the maximum field-size and dose-rate differences. Cassette orientation was therefore among the largest contributors to variation when beam incidence could not be reproduced between calibration and measurement.

DISCUSSION

This investigation characterized nanoDot OSLDs across conventional therapeutic photon beams. Principal findings were detector-specific sensitivity variation requiring ECF assignment, linear response through 300 cGy, beam-dependent supralinearity at higher doses, close chamber agreement for field size and dose rate, good reproducibility, detector-history effects, readout depletion, and angular variation reaching 6%. Together, the results show that nanoDots can support point-dose verification when calibration, readout, reuse, and orientation match the intended application. Each control addresses a distinct contributor to measurement uncertainty during clinical implementation.

The coefficients of determination confirm a linear interval between 50 and 300 cGy but do not justify extrapolation beyond it. At 1,000 cGy, supralinearity factors reached 1.46, indicating that an unchanged linear calibration could bias the derived dose. Work with Al_2O_3:C OSLDs in ultra-high-dose-rate proton beams also emphasizes validation under intended dose and delivery conditions.[13] High-dose applications should therefore use a validated nonlinear calibration or remain outside the claimed operating range. Electron-beam investigations likewise show that OSL response at ultra-high dose rate must be characterized against appropriate reference detectors.[14]

The ECF distribution demonstrates why batch calibration alone is insufficient. Values from 0.91 to 1.08 indicate that identically exposed detectors can produce different uncorrected signals. Applying an individual ECF converts this variation into a controlled term. This is especially important in nonstandard environments; measurements around a 1.5-T MR-linac show that OSLDs can support out-of-field assessment when response and setup are commissioned.[15] ECFs should be reviewed whenever detector history, bleaching performance, reader behavior, or quality-control measurements suggest drift.

Field-size and dose-rate effects were small, with OSLD–chamber differences below 2%. This supports ordinary clinical output measurements after local commissioning but does not demonstrate universal energy or geometry independence. Surface and near-surface MR-linac measurements show that detector placement, buildup, and magnetic-field conditions can alter response.[16] The cassette also changes attenuation and buildup. Grouping of the two 6-MV platforms prevents a separate platform-specific claim and should be clarified before publication.

Detector reuse requires attention. Although immediate inter-detector variation remained below 1.06%, bleaching and accumulated-dose histories produced differences of 8%–9%. Repeated analysis caused cumulative loss up to 18% after 200 readings. Two-dimensional OSL systems used in ultra-high-dose-rate electron beams similarly depend on controlled stimulation, calibration, and repeatability.[17] Routine measurements involve fewer readings, but the reading number should be recorded for serial analyses or verification repeats. A defined waiting interval, bleaching procedure, accumulated-dose limit, and periodic stability check are necessary.

Table 3: Summary of observed nanoDot OSLD performance and the corresponding operational controls supported by this study.

Characteristic	Reported finding	Practical control
Element sensitivity	ECF 0.91-1.08; 88% within ±5% of the mean	Apply an individual ECF before dose estimation
Dose response	Linear at 50-300 cGy; supralinear above 300 cGy	Use the linear calibration only within its validated range
Field size / dose rate	Maximum differences of 1.22%-1.60% and 1.8%, respectively	Commission under the intended beam quality and geometry
Reproducibility / reuse	Inter-detector variation <1.06%; history effect up to 8%-9%	Standardize bleaching and track accumulated dose
Repeated readout	0.06%-0.07% loss per read; cumulative loss up to 18%	Limit readings or apply a depletion correction
Angular response	Maximum deviation 5%-6%	Fix cassette orientation or use an angular correction

Clinical implications: For conventional fraction doses within the validated range, small size, passive operation, and repeat-read capability are practical advantages for phantom and selected in vivo measurements. High-resolution three-dimensional OSL research demonstrates the broader potential of luminescent materials for clinically relevant dose mapping.[18] For nanoDots, a defensible workflow should assign an ECF, document accumulated dose, standardize bleaching, limit repeated readout, reproduce orientation, and use the beam quality and geometry employed during calibration. [Table 3] translates measured characteristics into operational controls.

Angular response is relevant for surface or in vivo measurements because beam incidence may differ between calibration and treatment. The observed 5%–6% range approaches common point-dose action levels and exceeded field-size and dose-rate effects. Proton-therapy research has extended OSLDs to simultaneous point-dose and dose-weighted linear-energy-transfer assessment, illustrating their versatility and dependence on application-specific calibration.[19] Orientation markings, reproducible holders, and local angular corrections should therefore be considered whenever normal incidence cannot be maintained in practice.

Limitations: Interpretation is limited by the absence of detector-level data, complete replicate counts, uncertainty budgets, confidence intervals, and formal statistical comparisons. The available records differ on whether 100 or 200 detectors were used for ECF determination, although Figure 4 clearly identifies 200. Several experiments did not separate the two 6-MV platforms, and reproducibility reporting covered fewer beams than the methods described. Recent OSL film development shows how Monte Carlo modeling and energy-response optimization can strengthen characterization.[20] Detector count, platform grouping, replicate information, and uncertainty components must be reconciled with laboratory records before submission or clinical translation.

CONCLUSION

This phantom-based study demonstrates that Al_2O_3:C nanoDot OSLDs can provide sensitive and reproducible point-dose measurements in ^{60}Co and megavoltage photon beams when their known response dependencies are controlled. Element correction factors ranged from 0.91 to 1.08, confirming that individual sensitivity correction is necessary before comparing detectors or converting signal to dose. Within 50-300 cGy, dose response was strongly linear for every evaluated beam, with coefficients of determination above 0.99. This interval is therefore the most defensible range for a simple linear calibration based on the reported data.

Performance outside that controlled range was not invariant. Response became supralinear above 300 cGy, and the effect increased to factors between 1.21 and 1.46 at 1,000 cGy. Field-size and dose-rate dependence remained comparatively small, with maximum stated differences below 2%, while immediate inter-detector variation was below 1.06%. However, bleaching and accumulated-dose history altered response by as much as 8%-9%. Repeated optical stimulation depleted the stored signal, producing cumulative losses up to 18% after 200 readings. Cassette orientation also caused deviations of 5%-6%, exceeding the reported field-size and dose-rate effects.

Accordingly, clinical or research use should be supported by local commissioning that matches beam quality, dose range, phantom geometry and readout conditions. The operating procedure should assign and periodically review individual ECFs, define a post-irradiation waiting interval, standardize optical bleaching, track accumulated detector dose, specify the allowed number of readings and maintain a reproducible cassette orientation. High-dose measurements require a validated nonlinear correction rather than extrapolation of the conventional-dose calibration. Before publication or routine implementation, the unresolved detector count, beam-platform grouping, replicate information and uncertainty budget should be reconciled with the original laboratory records. With these controls, nanoDot OSLDs are promising for radiotherapy phantom dosimetry and carefully commissioned in vivo point-dose verification and research.

REFERENCES

1. Kry SF, Alvarez P, Cygler JE, DeWerd LA, Howell RM, Meeks S, O'Daniel J, Reft C, Sawakuchi G, Yukihara EG, Mihailidis D. AAPM TG 191: Clinical use of luminescent dosimeters: TLDs and OSLDs. Medical physics. 2020 Feb;47(2):e19-51.
2. Yukihara EG, Kron T. Applications of optically stimulated luminescence in medical dosimetry. Radiation Protection Dosimetry. 2020 Nov;192(2):122-38.
3. Yukihara EG, Bos AJ, Bilski P, McKeever SW. The quest for new thermoluminescence and optically stimulated luminescence materials: Needs, strategies and pitfalls. Radiation Measurements. 2022 Nov 1;158:106846.
4. Damulira E, Yusoff MN, Omar AF, Mohd Taib NH. A review: photonic devices used for dosimetry in medical radiation. Sensors. 2019 May 14;19(10):2226.
5. Rejab M, Wong JH, Jamalludin Z, Jong WL, Malik RA, Wan Ishak WZ, Ung NM. Dosimetric characterisation of the optically-stimulated luminescence dosimeter in cobalt-60 high dose rate brachytherapy system. Australasian Physical & Engineering Sciences in Medicine. 2018 Jun;41(2):475-85.
6. Ponmalar R, Manickam R, Saminathan S, Ganesh KM, Raman A, Godson HF. Evaluation of optically stimulated luminescence dosimeter for exit dose in vivo dosimetry in radiation therapy. Journal of Cancer Research and Therapeutics. 2018 Oct 1;14(6):1341-9.
7. Kim TJ, Jung KO, Fahimian B, Pratx G. Flexible optically stimulated luminescence band for 1D in vivo radiation dosimetry. Physics in Medicine & Biology. 2018 Aug 1;63(16):165006.
8. Han SC. Preliminary study for dose evaluation depending on dose range with optically stimulated luminescence dosimeter considering individual dosimeter sensitivity. Plos one. 2022 Mar 29;17(3):e0266110.
9. Choi Y, Sung J, Park K, Lee H. Dosimetric calibration of nanodot optically stimulated luminescent dosimeter for intraoperative radiotherapy with low-energy X-rays. Journal of the Korean Physical Society. 2022 Dec;81(11):1100-6.
10. Ito S, Araki F, Hoshida K, Ohno T. Impact of transverse magnetic fields on dose response of a nanoDot OSLD in megavoltage photon beams. Physica Medica. 2020 Feb 1;70:153-60.
11. Ando M, Hayashi H, Goto S, Yamaguchi H, Shimizu M. Beam quality conversion factor of BeO-OSLD for high-energy photon beams. Radiation Measurements. 2024 Jul 1;175:107164.
12. Kumar P, Sharma SD, Dhabekar B, Rawat NS, Mishra DR, Chaudhari S, Chandola RM, Routh T, Agrawal S. Multi-institutional dose audit in radiotherapy facilities using in-house developed optically stimulated luminescence disc

dosimeters. Journal of Cancer Research and Therapeutics. 2023;19(Suppl 1):S361-7.
13. Christensen JB, Togno M, Nesteruk KP, Psoroulas S, Meer D, Weber DC, Lomax T, Yukihara EG, Safai S. Al2O3: C optically stimulated luminescence dosimeters (OSLDs) for ultra-high dose rate proton dosimetry. Physics in Medicine & Biology. 2021 Apr 21;66(8):085003.
14. Motta S, Dal Bello R, Christensen JB, Bossin L, Yukihara EG. Dosimetry of ultra-high dose rate electron beams using thermoluminescence and optically stimulated luminescence detectors. Physics in Medicine & Biology. 2024 Feb 7;69(3):035022.
15. Zhang Y, Yan S, Cui Z, Wang Y, Li Z, Yin Y, Li B, Quan H, Zhu J. Out-of-field dose assessment for a 1.5 T MR-Linac with optically stimulated luminescence dosimeters. Medical Physics. 2021 Jul;48(7):4027-37.
16. Kim A, Lim-Reinders S, Ahmad SB, Sahgal A, Keller BM. Surface and near-surface dose measurements at beam entry and exit in a 1.5 T MR-Linac using optically stimulated luminescence dosimeters. Physics in Medicine & Biology. 2020 Feb 1;65(4):045012.
17. Vanreusel V, Gasparini A, Galante F, Mariani G, Pacitti M, Colijn A, Reniers B, Yalvac B, Vandenbroucke D, Peeters M, Leblans P. Optically stimulated luminescence system as an alternative for radiochromic film for 2D reference dosimetry in UHDR electron beams. Physica Medica. 2023 Oct 1;114:103147.
18. Jensen ML, Julsgaard B, Turtos RM, Skyt PS, Jensen MB, Muren LP, Balling P. High-resolution three-dimensional dosimetry in clinically relevant volumes utilizing optically stimulated luminescence. Medical Physics. 2024 Mar;51(3):2200-9.
19. Bobić M, Christensen JB, Lee H, Choulilitsa E, Czerska K, Togno M, Safai S, Yukihara EG, Winey BA, Lomax AJ, Paganetti H. Optically stimulated luminescence dosimeters for simultaneous measurement of point dose and dose-weighted LET in an adaptive proton therapy workflow. Frontiers in Oncology. 2024 Jan 8;13:1333039.
20. De Saint-Hubert M, Caprioli M, de Freitas Nascimento L, Delombaerde L, Himschoot K, Vandenbroucke D, Leblans P, Crijns W. New optically stimulated luminescence dosimetry film optimized for energy dependence guided by Monte Carlo simulations. Physics in Medicine & Biology. 2024 Apr 7;69(7):075005.